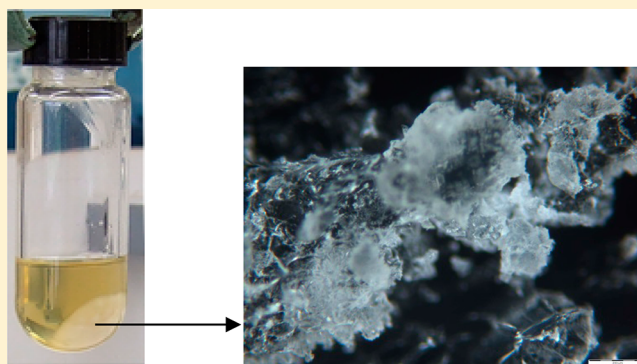


Liquid/Gas and Liquid/Liquid Phase Equilibria of the System Water/  
Bovine Serum AlbuminYurij Antonov,<sup>†</sup> John Eckelt,<sup>‡,§</sup> Rei Sugaya,<sup>||</sup> and Bernhard A. Wolf<sup>\*,‡,§</sup><sup>†</sup>N. M. Emanuel Institute of Biochemical Physics, Russian Academy of Sciences, Kosygin Str. 4, 119334 Moscow, Russia<sup>‡</sup>Institut für Physikalische Chemie der Johannes Gutenberg-Universität Mainz, Welder-Weg 11, D-55099 Mainz, Germany<sup>§</sup>WEE-Solve GmbH, Auf der Burg 6, D-55130 Mainz, Germany<sup>||</sup>Japan Science and Technology Agency (JST) 4-1-8, Honcho, Kawaguchi-shi, Saitama, 332-0012 Japan

**ABSTRACT:** The thermodynamic behavior of the system H<sub>2</sub>O/BSA was studied at 25 °C within the entire composition range: vapor pressure measurements via head space sampling gas chromatography demonstrate that the attainment of equilibria takes more than one week. A miscibility gap was detected via turbidity and the coexisting phases were analyzed. At 6 °C the two phase region extends from ca. 34 to 40 wt % BSA; it shrinks upon heating. The polymer rich phase is locally ordered, as can be seen under the optical microscope using crossed polarizers. The Flory–Huggins theory turns out to be inappropriate for the modeling of experimental results. A phenomenological expression is employed which uses three adjustable parameters and describes the vapor pressures quantitatively; it also forecasts the existence of a miscibility gap.



## 1. INTRODUCTION

Despite the long-standing engagement in the thermodynamics of polymer containing liquids our knowledge in some interesting and biologically important areas is still rudimentary. One such example concerns the phase separation behavior of joint solutions of different types of polymers. This statement does not imply the absence of research on such systems; numerous studies have been performed on biological systems as described in several overviews.<sup>1–7</sup> The difficulty with the reported knowledge lies in the fact that it refers to biological systems, which are by nature very complex and contain a multitude of different components.

For a more comprehensive understanding of the above-mentioned multinary systems it appears mandatory to dispose of reliable information concerning the thermodynamic behavior of the corresponding binary subsystems. Only under this condition it is for instance possible to assess whether the interactions between the different components observed in binary mixtures remain unchanged in the case of a higher number of components or whether special interactions between two or more solutes change the behavior fundamentally. This situation has become very clear to us when we wanted to interpret ongoing experiments with the ternary system water/dextran/bovine serum albumin (H<sub>2</sub>O/DEX/BSA). For that reason we searched for information concerning aqueous solutions of the two types of polymers. In the case of H<sub>2</sub>O/DEX the required data have already been published,<sup>8</sup> in contrast to the subsystem H<sub>2</sub>O/BSA, for which we could not

find the required information. This is the reason why we have conducted the study reported here.

## 2. EXPERIMENTAL SECTION

**2.1. Materials.** BSA, Fraction V, pH 5 (Lot A018080301), was obtained from Across Organics Chemical Co. (protein content = 98–99%; trace analysis, Na < 5000 ppm, Cl < 3000 ppm, no fatty acids detectible). According to the literature<sup>9</sup> the molar mass of BSA is 66.4 kDa. The isoelectric point of the protein amounts to 4.8–5.0 and the radius of gyration<sup>10</sup> at pH 5.3 is 30.6 Å. Millipore-quality water was used throughout the experiments. All measurements were performed at pH 5.4, because serum albumin undergoes conformational isomerization and changes in the conformation state and secondary structure with changes in pH from pH 5–5.5 to acid and alkaline region.<sup>10</sup> The extinction of 1% BSA solution at 279 nm was  $A_{279}^{1\%} = 6.70$ ; this value is very close to the tabulated value<sup>11</sup> of 6.67.

**2.2. Solution Preparation.** To prepare BSA stock solutions, the biopolymer was gradually added to the deionized water and stirred at 298 K for 2 h. The solutions were then centrifuged at 13 000g for 1 h at 298 K to remove insoluble particles. Subsequently, the concentration of the biopolymer was determined by measuring the dry weight residue. The content of protein nitrogen in the dry BSA samples was always

Received: January 30, 2013

Revised: April 5, 2013

Published: April 11, 2013

taken into account calculating the concentration of protein in solution. In some cases, the final protein concentration was determined also by spectrophotometric measurements.

**2.3. Vapor Pressures.** Vapor pressure measurements were carried out as described in the literature<sup>12</sup> for volume fractions  $\phi$  of the polymer up to 0.968 by means of an apparatus consisting of the headspace-sampler Dani HSS 3950, Milano (Italy) and a gas chromatograph Shimadzu GC 14B, Kyoto (Japan). In these measurements a constant volume of the equilibrium vapor phase is taken out of sealed vials by means of a syringe through a septum and analyzed in a gas chromatograph. In this manner it is possible to calculate the partial vapor pressures of the volatiles. No corrections for imperfections of the gas were necessary with the present systems to obtain fugacities. In all cases we made allowance for the amount of gas that is contained in the vapor phase, when calculating the composition of the liquid mixture. In order to promote the attainment of equilibria at high polymer concentrations we have prepared thin films (5 to 20  $\mu$  m thick) on glass beads of 4 mm diameter. To this end the voids between the beads were filled with a sufficiently viscous aqueous solution of BSA (ca. 20 wt %) and the desired final composition of the solutions was established stripping off the excess solvent at room temperature by applying vacuum. For the highest concentrations the solvent was totally removed and then the dry films were either loaded with water via the gas phase or by adding the required amount of liquid water. The establishment of equilibria was checked by measuring the vapor pressures as a function of time up to three weeks. For organic solvents the error of the vapor pressures is typically on the order of 1%–2%; with the present aqueous solutions the errors are markedly larger, particularly in the range of low  $\phi$  values as indicated in Figure 1.

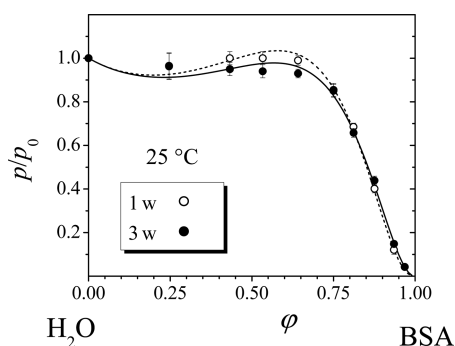


**Figure 1.** Reduced vapor pressures as a function of polymer concentration (volume fractions) for different equilibration times. The curves are calculated by means of eq 4 plus the parameters specified in the legend of Figure 5.

**2.4. Phase Behavior.** Aqueous solutions containing approximately 25 wt % BSA were prepared by gradually adding the appropriate amount of the biopolymer to the deionized water under stirring at the temperature of interest. After 3 h the solutions were centrifuged at 13 000g for 1 h at the same temperature to remove insoluble particles. The BSA concentration in the thus obtained solutions was determined by measuring the dry weight residue.

Cloud-point concentrations were determined by removing water from 24.5 wt % solutions of BSA at constant temperature. To this end the solutions were kept in open vials in a thermostat and stirred until the liquids became turbid. Depending on temperature this procedure took 18–36 h.

Stripping off more solvent leads to the segregation of a polymer rich phase; its separation by centrifugation and the analysis of the coexisting phases yields the tie lines of the system at the given temperature. The BSA rich phase appears slightly opaque and was therefore inspected under the Olympus CX31-P polarized light microscope.

### 3. RESULTS

**3.1. Vapor Pressures.** Figure 1 shows how the reduced vapor pressure of water ( $p/p_0$ , where  $p_0$  is the vapor pressure of pure water) decreases as the volume fraction,  $\phi$ , of BSA becomes larger. It also demonstrates a pronounced influence of time: Within some medium range of  $\phi$  values the vapor pressures decline upon standing; in order to reach equilibria one needs to wait at least 2 weeks. Both curves, the one for 1 week and the one for 3 weeks, exhibit extrema; this observation clearly indicates the existence of a miscibility gap between water and BSA: The vapor pressure may become identical for different polymer concentrations only if two liquid phases coexist.

The observed time dependence of the vapor pressures, most pronounced in the middle range of composition, is untypical for solutions of uncharged chain molecules. Slow equilibration of the present order was, however, observed when mixing dilute solutions of oppositely charged polyelectrolytes.<sup>13–15</sup> The molecular explanation is the following: After a first rapid step of equilibration, consisting in contact formation between the two types of solutes, slow rearrangements are required to attain the minimum Gibbs energy of the system. It does not appear unreasonable to assume that similar processes are necessary to transfer parts of the BSA molecule that interact most favorably with water to the outer regions. This reasoning is backed by the observation that the vapor pressures decrease with time, indicating an improvement in the thermodynamic quality of water for BSA. The explanation of why this effect dies out at very dilute and very concentration mixtures is trivial. On one end of the composition scale the pure solvent becomes dominant for the measured vapor pressure, and on the other end water will interact almost exclusively with the most favorable site of BSA, which may always be readily accessible.

**3.2. Demixing Behavior.** Indirect information concerning limitations in the miscibility of BSA and water obtained from the vapor pressure data were checked by directed experiments. The coexisting phases, segregated by centrifugation, look very different. The upper phase of lower BSA content flows readily, whereas the lower phase is highly viscous and has a gel like appearance; it is slightly opaque and exhibits a complex rheological behavior.

Figure 2 shows how the compositions of the coexisting phases vary with temperature. The BSA rich phase appears slightly turbid, in contrast to the BSA lean phase (cf. ToC graphic). Presently it is unclear whether the opaqueness of the gel phase is due to the establishment of microphase equilibrium (between ordered and disordered structures) or the consequence of incomplete macroscopic phase separation (occlusion of parts of the coexisting sol phase). The fact that the miscibility gap narrows as  $T$  rises indicates endothermal mixing of the components. This graph also displays the measured cloud points and demonstrates that they do not fall on the coexistence curve. In view of the experimental procedure it is highly probable that they represent spinodal points. Due to the extensive purification of the starting BSA solutions the concentration of nuclei, promoting the segregation of a second

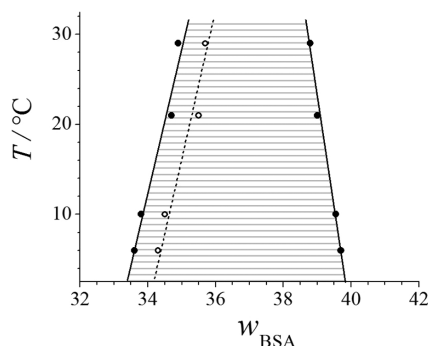


**Figure 2.** Phase diagram of the system H<sub>2</sub>O/BSA. (Full circles) Composition of the coexisting phases and (open circles) spinodal points (cf. text).

phase, is expected to be very low. This means that the homogeneous mixtures do not demix when crossing stability limits upon the stripping of water and increasing the BSA concentrations. Instead they remain one phase within the metastable regime. It is only at the border between metastability and instability that phase separation becomes inevitable and the solutions get turbid. In other words, the temperature/composition range located in the phase diagram between the left-hand branch of the coexistence curve and the dotted line represents the metastable region.

A closer inspection of the BSA rich coexisting phase under crossed polarizers reveals the existence of ordered regions; Figure 3 shows a typical example of these images.

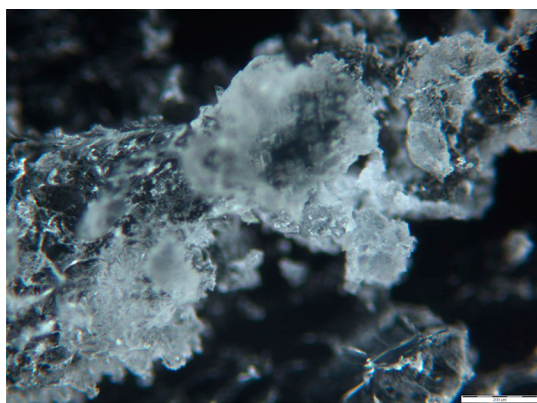


**Figure 3.** Micrograph of the BSA rich coexisting phase; the bar indicates 200 μm. The bright parts indicate the ordered regions of the solution.

#### 4. DISCUSSION

The Flory–Huggins theory<sup>16</sup> acquires the parameter  $\chi$  from experimental data on the reduced vapor pressures of the solvent according to the following relation:

$$\ln \frac{p}{p_0} = \chi \varphi^2 + \ln(1 - \varphi) + \left(1 - \frac{1}{N}\right) \varphi \quad (1)$$

$\varphi$  stands for the volume fraction of the polymer,  $N$  is the number of polymer segments (normally the ratio of the polymer molar volume divided by the molar volume of the solvent),  $p$  is the vapor pressure at a given value of  $\varphi$ , and  $p_0$  is that of the pure solvent. In the general case  $\chi$  depends markedly on  $\varphi$ , which means that the integral Flory–Huggins interaction

parameter  $g$  (required for instance for the calculation of phase diagrams) is not identical with  $\chi$ . Knowing  $\chi(\varphi)$ , the integral parameter is accessible via the expression

$$g = -\frac{1}{1 - \varphi} \int_1^\varphi \chi(\varphi) d\varphi \quad (2)$$

Figure 4 shows the Flory–Huggins interaction parameter  $\chi$  as a function of composition, calculated according to eq 1 from the

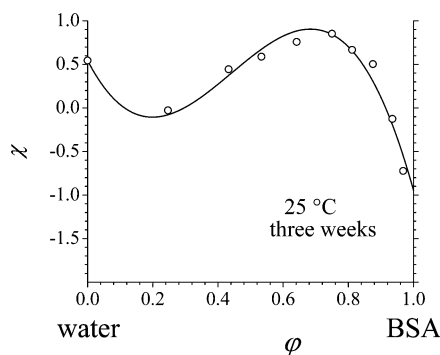


**Figure 4.** Composition dependence of interaction parameter water/BSA obtained from the measured vapor pressures according to eq 1. The data point for vanishing polymer concentration stems from light scattering measurements. The curve is modeled by means of a series expansion of  $\chi$  (cf. eq 3) up to  $i = 3$  ( $\chi_0 = 0.545$ ,  $\chi_1 = -7.242$ ,  $\chi_2 = 23.50$ , and  $\chi_3 = -17.75$ ).

vapor pressure measurement after 3 weeks of equilibration. The curve shown in this graph is modeled by means of the following series expansion of  $\chi$

$$\chi = \sum_{i=0}^n \chi_i \varphi^i \quad (3)$$

For most polymer solutions it suffices to account for three terms ( $i = 2$ ); however, in the present case we had to use one more.

The main problem with the evaluation along the traditional routes outlined above lies in the fact that the present solute is a globular macromolecule and that approaches developed for chain molecules are inadequate by nature. The modeling remains rather inaccurate even if higher members of the series expansion are included and it does not predict the experimentally observed phase equilibria. Considerations similar to the ones described above also hold true for the application of a newer approach<sup>15</sup> eliminating some deficiencies of the original Flory–Huggins theory. This can for instance be seen from the fact that the normally concentration independent parameter  $\nu$  of this approach (accounting for the different surfaces of solvent molecules and polymer segments) must be treated as concentration dependent in order to model the present results with similar quality as the Flory–Huggins theory. Flory's theory for stiff rods<sup>17</sup> as well as the theory of Semenov and Rubinstein<sup>18</sup> fail too.

For the reasons described above we have worked out a purely phenomenological approach,<sup>19</sup> which is also capable of modeling solutions of globular or charged macromolecules. The relation for the composition dependence of the vapor pressures corresponding to eq 1 reads



$$\ln \frac{p}{p_0} = (z - k)\varphi + b\varphi^2 + c\varphi^2(1 - 2\varphi) + z \ln(1 - \varphi) \quad (4)$$

where the parameter  $k$  is calculated from the molar mass  $M$  of the polymer and its density  $\rho$  plus the molar volume of the solvent according to

$$k = \frac{\bar{V}_1 \rho}{M} \quad (5)$$

The parameters  $b$  and  $c$  originate from a series expansion of the Gibbs energy of mixing;  $b$  quantifies binary interactions solvent/polymer and  $c$  ternary interactions of the type solvent/polymer/polymer. Formally the inverse of the parameter  $z$  corresponds to an effective number of solvent segments, which is in the Flory–Huggins theory by definition set equal to unity.

The curves connecting the measured vapor pressure data in Figure 5 are modeled by means of eq 4 adjusting the

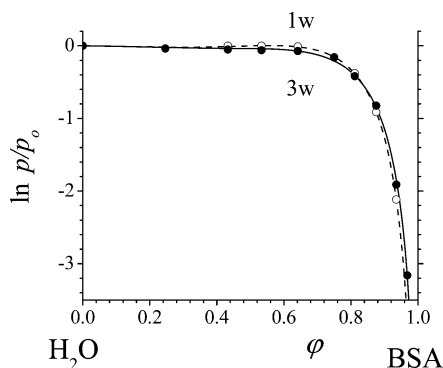


**Figure 5.** Evaluation of the composition dependent reduced vapor pressures according to eq 4. For 1 week the parameters are  $b = 2.26$ ,  $c = -1.57$ , and  $z = 2.94$ , and for 3 weeks they are  $b = 1.68$ ,  $c = -1.25$ , and  $z = 2.36$  ( $k = 2.7 \times 10^{-4}$  in both cases).

parameters  $b$ ,  $c$ , and  $z$ . This graph demonstrates that despite the use of three parameters only (instead of four in the case of the series expansion) the functions deviate less from the data points.

In the following we check to which extent the thermodynamic information acquired from vapor pressures can model the observed phase behavior. To that end it is not only necessary to know the Gibbs energy of dilution (eq 4) but also the corresponding Gibbs energy of mixing,  $\Delta\bar{G}$ . For the present approach this relation reads<sup>19</sup>

$$\frac{\Delta\bar{G}}{RT} = z(1 - \varphi) \ln(1 - \varphi) + k\varphi \ln \varphi + b\varphi(1 - \varphi) - c(1 - \varphi)\varphi^2 \quad (7)$$

The easiest way to recognize the existence or absence of miscibility gaps is provided by the calculation of the spinodal conditions (e.g., the limits between metastability and instability of the mixture). Under these circumstances the second derivative of  $\Delta\bar{G}$  with respect to  $\varphi$  becomes zero. From eq 7 one obtains the following expression:

$$\frac{\partial^2(\Delta\bar{G}/RT)}{\partial\varphi^2} = -2(b + c) + \frac{k}{\varphi} + \frac{z}{1 - \varphi} + 6c\varphi \quad (8)$$

Figure 6 displays the second derivatives calculated by means of the parameters following from the vapor pressure data (cf.

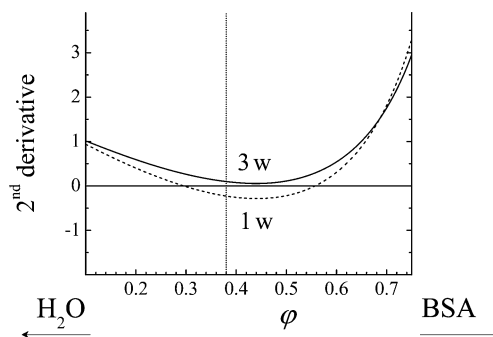


**Figure 6.** Second derivative of the Gibbs energy of mixing as a function of composition calculated according to eq 8 with the parameters of Figure 5; the dotted vertical line displays the center of the experimentally observed miscibility gap.

legend of Figure 4). According to the broken curve (equilibration of one week) the system  $\text{H}_2\text{O}/\text{BSA}$  should be unstable within the composition range from  $\varphi \approx 0.3$  to  $0.56$ ; this prediction exaggerates the extension of the miscibility gap considerably. It does, however, not yet refer to equilibrium conditions, which are prevailing after 3 weeks. Figure 6 shows these data by the full line, which comes very close to zero but does not fall below this value. Because of the necessity to integrate and to differentiate twice in order to obtain eq 8, this result is too uncertain to conclude that the system homogenizes upon standing. The shift in the second derivatives with time does, however, clearly indicate that the miscibility gap narrows during the equilibration period. This observation is consistent with the lower vapor pressures (more favorable interaction of the solvent with the polymer) after 3 weeks as compared with that for 1 week (Figure 1).

The phase behavior of the present system differs fundamentally from that observed with solutions of uncharged chain molecules by the fact that the polymer rich coexisting phase exhibits microscopic inhomogeneities as documented by the micrograph of Figure 3. Such pictures are typical for solutions of colloids or ionic solutes and have already been discussed extensively in the literature.<sup>20</sup> For the present case we assume that locally ordered volume elements lead to birefringence. According to the above cited investigations free particles are roughly speaking moving in a Brownian manner, whereas particles located within the ordered regions oscillate around their lattice point, the structure as a whole moving rather slowly. This situation implies that at least two diffusion processes exist: a fast one for free particles and a slow one for particles caught in ordered regions. It is the latter mode that could be responsible for the slow equilibration process observed in the context of the vapor pressure measurements.

For the discussion of the temperature influences on the extension of the miscibility gap shown in Figure 2, it would appear interesting to have a look at the heat effects associated with the formation of the ordered structures. Unfortunately such information is presently not available; according to theoretical considerations<sup>21</sup> the potential is not very deep, which means that thermal measurements need to be very accurate to yield reliable data. Conclusions based on the observed phase diagram (phase separation upon cooling) indicate moderate to small endothermal heats of mixing. This

seems to contradict structure formation, requiring that the loss of entropy is overcompensated by favorable exothermal heats of mixing. However, in view of the complexity of the present system, i.e. possible restructuring of the biopolymer and changes in the structure of water by the solute the above qualitative reasoning is not conclusive.

The observed microscopic inhomogeneities (birefringent parts of Figure 3) are according to the above discussion attributed to weak favorable interactions between the solute.<sup>20</sup> This line of reasoning implies that the ordered structures can be readily broken by shear. This inference is in good agreement with the pronounced shear thinning behavior observed with the present system.<sup>22–24</sup>

## 5. CONCLUSIONS

One central finding of the present vapor pressure measurements concerns their pronounced time dependence, which, to our knowledge, has not yet been reported for protein solutions. Such effects have, however, been observed when studying the formation of polyelectrolyte complexes,<sup>25</sup> where this phenomenon was attributed to slow rearrangements of the segments of the oppositely charged macromolecules. Analogous changes in the location of hydrophilic and hydrophobic parts of BSA are probably also required to attain the minima of the Gibbs energy.

The measured equilibrium vapor pressures yield the Gibbs energy of dilution as a function of composition. For solutions of chain molecules it is normally possible to describe them by means of the Flory–Huggins theory; for BSA this approach fails. Modeling attempts show that even a series expansion of four terms does not suffice. Moreover, the composition dependence of the Gibbs energy does not forecast the experimentally observed miscibility gap between water and BSA. These observations are, however, not surprising in view of the fact that BSA is a globular macromolecule, i.e., that the laws established for chain molecules become obsolete.

In view of the above-described impracticality of the Flory–Huggins theory we have designed a phenomenological approach, which is capable of reproducing the composition dependence of the measured chemical potential of the solvent by means of three adjustable parameters. This relation complies with all laws of thermodynamics and predicts the existence of a miscibility gap between the components. According to the available experimental information on other protein solutions and on polyelectrolyte solutions, the present approach is generally applicable.

## AUTHOR INFORMATION

### Notes

The authors declare no competing financial interest.

## ACKNOWLEDGMENTS

The authors are grateful to the DAAD and to the DFG for their support. Furthermore they thank the co-workers of Prof. R. Zentel (department of organic chemistry) for helping us with their microscopy experience.

## REFERENCES

(1) Albertsson, P. Å. *Partition of cell particles and macromolecules: Separation and purification of biomolecules, cell organelles, membranes, and cells in aqueous polymer two-phase systems and their use in biochemical analysis and biotechnology*, 3rd ed.; Wiley: New York, 1986; pp 15–346

(2) Antonov, Y. A.; Grinberg, V. Y.; Zhuravskaya, N. A.; Tolstoguzov, V. B. Liquid 2-Phase Water-Protein-Polysaccharide Systems and Their Processing into Textured Protein Products. *J. Texture Stud.* **1980**, *11*, 199–215.

(3) Grinberg, V. Y.; Tolstoguzov, V. B. Thermodynamic Incompatibility of Proteins and Polysaccharides in Solutions. *Food Hydrocolloid* **1997**, *11*, 145–158.

(4) Hill, S. E.; Ledward, D. A.; Mitchell, J. R. *Functional Properties of Food Macromolecules*, 2nd ed.; Aspen: Gaithersburg, MD., 1998; pp xvi, 348.

(5) Harding, S. E.; Hill, S. E.; Mitchell, J. R. *Biopolymer mixtures*; Nottingham University Press: Nottingham, U.K., 1995; pp XI, 499.

(6) Zaslavsky, B. Y. *Aqueous Two-phase Partitioning Physical Chemistry and Bioanalytical Applications*; M. Dekker: New York, 1995; p 696.

(7) Antonov, Y. A. Use of Membraneless Osmosis for Concentration of Proteins from Molecular-dispersed and Colloidal-dispersed Solutions (Review). *Appl. Biochem. Microbiol.* **2000**, *36*, 325–337.

(8) Eckelt, J.; Sugaya, R.; Wolf, B. A. Pullulan and dextran: Uncommon composition dependent Flory-Huggins interaction parameter of their aqueous solutions. *Biomacromolecules* **2008**, *9*, 1691–1697.

(9) Hirayama, K.; Akashi, S.; Furuya, M.; Fukuhara, K. Rapid Confirmation and Revision of the Primary Structure of Bovine Serum-Albumin by Esims and Frit-Fab Lc Ms. *Biochem. Biophys. Res. Commun.* **1990**, *173*, 639–646.

(10) Foster, J. F. *Albumin Structure, Function and Uses*; Pergamon: Oxford, U.K., 1977; pp 53–84.

(11) Kirschenbaum, D. M. Molar Absorptivity and a-1-Percent-1-Cm Values for Proteins at Selected Wavelengths of UV and Visible Regions 0.13. *Anal. Biochem.* **1977**, *81*, 220–246.

(12) Petri, H.-M.; Wolf, B. A. Concentration Dependent Thermodynamic Interaction Parameters for Polymer solutions: Quick and Reliable Determination via Normal Gas Chromatography. *Macromolecules* **1994**, *27*, 2714–2718.

(13) Zintchenko, A.; Rother, G.; Dautzenberg, H. Transition Highly Aggregated Complexes-Soluble Complexes Via Polyelectrolyte Exchange Reactions: Kinetics, Structural Changes, and Mechanism. *Langmuir* **2003**, *19*, 2507–2513.

(14) Bakeev, K.; Izumrudov, V.; Kuchanov, S.; Zezin, A.; Kabanov, V. Kinetics and Mechanism of Interpolyelectrolyte Exchange and Addition-Reactions. *Macromolecules* **1992**, *25*, 4249–4254.

(15) Bercea, M.; Nichifor, M.; Eckelt, J.; Wolf, B. A. Dextran-Based Polycations: Thermodynamic Interaction With Water as Compared With Unsubstituted Dextran 2, Flory/Huggins Interaction Parameter. *Macromol. Chem. Phys.* **2011**, *212*, 1932–1940.

(16) Koningsveld, R.; Stockmayer, W. H.; Nies, E. *Polymer Phase Diagrams: A Textbook*; Oxford University Press: New York, 2001; pp xvii, 341.

(17) Flory, P. J.; Ronca, G. Theory of Systems of Rodlike Particles 0.2. Thermotropic Systems with Orientation-Dependent Interactions. *Mol. Cryst. Liq. Cryst.* **1979**, *54*, 311–330.

(18) Rubinstein, M.; Semenov, A. N. Thermoreversible Gelation in Solutions of Associating Polymers. 2. Linear Dynamics. *Macromolecules* **1998**, *31*, 1386–1397.

(19) Wolf, B. A. Unified Thermodynamic Modeling of Polymer Solutions: Polyelectrolytes, Proteins, and Chain Molecules. *Ind. Eng. Chem. Res.* **2013**, in press.

(20) Hatters, D. M.; Minton, A. P.; Howlett, G. J. Macromolecular Crowding Accelerates Amyloid Formation by Human Apolipoprotein C-II. *J. Biol. Chem.* **2002**, *277*, 7824–7830.

(21) Sogami, I.; Ise, N. On the Electrostatic Interaction in Macroionic Solutions. *J. Chem. Phys.* **1984**, *81*, 6320–6332.

(22) Lefebvre, J.; Riot, A.-S. Rheological Evidence for Large Scale Structure in Moderately Concentrated Ionic Protein Solutions. *Conference proceedings 1st International Symposium on Food Rheology and Structure*; Swiss Federal Institute of Technology: Zurich, Switzerland, 1997; pp 175–179.

(23) Ikeda, S.; Nishinari, K. Intermolecular Forces in Bovine Serum Albumin Solutions Exhibiting Solidlike Mechanical Behaviors. *Biomacromolecules* **2000**, *1*, 757–763.

(24) Sharma, V.; Jaishankar, A.; Wang, Y.-C.; McKinley, G. H. Rheology of Globular Proteins: Apparent Yield Stress, High Shear Rate Viscosity and Interfacial Viscoelasticity of Bovine Serum Albumin Solutions. *Soft Matter* **2011**, *7*, 5150–5160.

(25) Bercea, M.; Nita, L.-E.; Eckelt, J.; Wolf, B. A. Polyelectrolyte Complexes: Phase Diagram and Intrinsic Viscosities of the System Water/Poly(2-vinylpyridinium-Br)/(Poly(styrene sulfonate-Na)). *Macromol. Chem. Phys.* **2012**, *213*, 2504–2513.